RSC Advances

ROYAL SOCIETY OF CHEMISTRY

www.rsc.org/advances

Journal Name

RSCPublishing

ARTICLE

Mediating Ordered Assembly of Gold Nanorods by Controlling Droplet Evaporation Modes for Surface Enhanced Raman Scattering

Cite this: DOI: 10.1039/x0xx00000x

Received 00th January 2012,
Accepted 00th January 2012

DOI: 10.1039/x0xx00000x

www.rsc.org/

Young-Kwan Kim, Hee-Kyung Na, Seulbeom Ham and Dal-Hee Min*

The evaporation induced self-assembly of nanomaterials has emerged as one of the important approaches to fabricate various ordered nanostructures with enhanced optical properties. In this study, gold nanorods (GNRs) were selected as a building block and investigated for the droplet evaporation induced self-assembly of GNRs by using self-assembled monolayers (SAMs) as a tool to control droplet evaporation mode. By controlling the droplet evaporation mode of colloidal GNRs, the large scale ordered assemblies of GNRs were successfully fabricated with significantly enhanced collective optical properties such as two photon luminescence (TPL) and surface enhanced Raman scattering (SERS). The confined ordered assemblies of GNRs was also achieved on a pre-designated region through the combination of surface-mediated droplet evaporation with soft lithography and/or mass spectrometry assisted lithography.

Introduction

The self-assembly of colloidal nanocrystals into ordered structure has attracted much attention from various research fields such as surface enhanced spectroscopies,[1] sensors,[2] photovoltaics[3] and optoelectronics[4] because ordered assembly structures could provide many collective interactions between each nanocrystal to significantly enhance their own functional properties. Therefore, many effort have been devoted to develop appropriate self-assembly strategies to fabricate supercrystalline structures such as dry manual,[5] interfacial,[6] and droplet evaporation assembly[7] as well as Langmuir-Blodgett deposition.[8] Among those strategies, the droplet evaporation assembly has been extensively investigated because of its simplicity, cost-effectiveness and wide applicability to various functional nanomaterials. Especially, GNRs (GNRs) have attracted increasing attention as a building block of supercrystalline structures through droplet evaporation self-assembly based on their collective surface plasmon resonance (SPR) property significantly dependent on their orientation, inter-particle distance, and local density.[9-11] In this regard, the ordered assembly of GNRs are closely related to maximizing surface plasmon coupling for electromagnetic enhancement of surface enhanced Raman scattering (SERS) to develop an efficient biochemical sensing platform.[12]

Previously, Ming et al. reported ordered assembly of gold nanomaterials with various shapes such as rod, polyhedra, nanocube, and bipyramid by droplet evaporation on silicon substrates. They observed the formation of shape dependent ordered assembly along the edge of droplet and the enhanced two photon luminescence of the ordered assembly structures of GNRs on the substrate.[13] Several approaches have been employed to control assembly and fabricate ordered structures of GNRs, such as adjusting the concentration of the nanomaterial suspension, adding organic molecules,[14-16] humidity and temperature,[17] exchanging surface ligands[18-22] or using nanostructured substrate.[23] However, the formation of such ordered assemblies of GNRs was limited along the edge of droplet with narrow width or locally patterned regions in nanoscale. Therefore, it is an urgent issue to develop an efficient strategy for fabrication of large scale ordered assemblies of GNRs and their applications as biochips and sensor arrays.

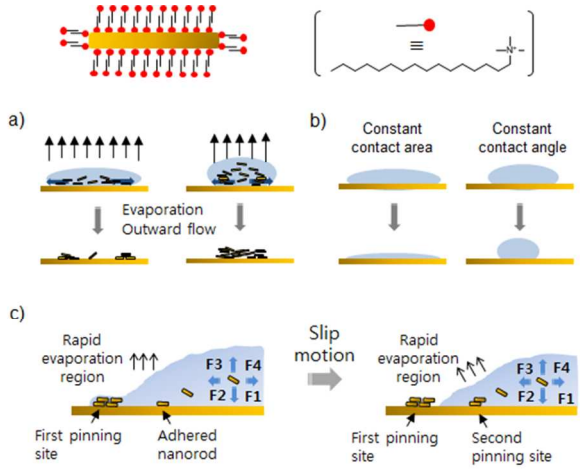

Scheme 1 Structure of CTAB stabilized GNRs (top), solvent evaporation-induced formation of ordered assemblies of GNRs on hydrophilic and hydrophobic surfaces (a), different evaporation modes according to the surface wettability,(b) and process of multiple coffee ring formation and forces that control ordered assembly of GNRs in droplet evaporation induced self-assembly (c).

Herein, we report a strategy of mediating the formation of ordered assemblies of GNRs by controlling droplet evaporation mode of colloidal GNRs (Scheme 1a). To the best of our knowledge, it is the first example to fabricate ordered assemblies of GNRs on chemically functionalized surfaces by controlling the droplet evaporation mode of colloidal GNRs. To control the droplet evaporation mode of colloidal GNRs, we harnessed self-assembled monolayers (SAMs) presenting different functional groups on gold-coated substrates.[24] Droplets of colloidal GNRs were expected to be held to the substrate surfaces by different interfacial tensions, which resulted in differences in the evaporation mode and rate of solvent[25-27] with varying local concentration of GNRs at the edge of each droplet.

Especially, the evaporation mode of water droplet is significantly influenced by initial contact angle. When the initial contact angle is smaller than 90°, the evaporation rate is linear and follows constant contact area mode. By contrast, with the initial contact angle over 90°, the evaporation rate is nonlinear and follows the constant contact angle mode (Scheme 1b).[28] The control of evaporation mode by surface functionalization was expected to mediate the formation of large scale ordered assemblies of GNRs as shown in scheme 1b. The fabricated ordered assemblies of GNRs showed considerable enhancement of their collective optical properties such as TPL and SERS depending on their droplet evaporation mode. Based on the understanding of assembly behaviour of colloidal GNRs on the various SAMs, we further fabricated patterns of assembled GNRs on the substrates covered by patterned SAMs with a pre-designed shape, presenting functional groups of choice to fabricate arrays of efficient SERS platform.

Experimental

Materials

Gold substrates were prepared by vacuum deposition of titanium (5 nm) followed by gold (50 nm) onto glass wafer (500 μm in thickness). Hydrogen tetrachloroaurate(III) hydrate was purchased from Kojima chemicals (Japan). Cetyltrimethylammonium bromide (CTAB) was purchased from Acros (New Jersey, USA). Ethanol was purchased from Merck (Darmstadt, Germany). Hexadecanethiol (HDT), 11-amino-1-undecanethiol hydrochloride (AUT), siliver nitrate, ascorbic acid, 4-aminothiophenol (4-ATP) and other reagents were purchased from Sigma-Aldrich (St. Louis, MO, USA). Alkanethiol presenting triethylene glycol terminal groups, (11-mercaptoundecyl)tri(ethylene glycol) (ATG) was synthesized by previously reported procedure.[29]

Preparation of SAMs

The gold substrate was cleaned in Piranha solution (sulfuric acid: hydrogen peroxide (30%) = 70:30, WARNING: Piranha solution is highly corrosive and reactive. Handle with caution.) for 10 min, washed with deionized water and ethanol, and dried under a nitrogen stream. The cleaned substrates were respectively immersed in 1 mM ethanolic solutions of different alkane thiols such as ATG, AUT and HDT presenting EG_3, NH_2 and CH_3 terminal groups for 12 h. The substrates were rinsed with ethanol and dried under a stream of nitrogen.

Preparation of line patterned SAMs

For line patterns of ordered assemblies, the line patterned (100 μm in width) PDMS elastomers were rinsed with ethanol and dried under a stream of nitrogen prior to use. The elastomer was rubbed by a Q-tip soaked with 1 mM ethnolic solution of hexadecanethiol and dried under a stream of nitrogen. The piranha treated gold substrates were placed on the inked elastomer with light pressure for 30 sec. The gold substrate was immediately immersed into 1 mM ethanolic solutions of alkanethiol presenting EG_3 terminal groups for 1 h, rinsed with water and ethanol and dried under a stream of nitrogen.

Preparation of octagon patterned SAMs

The SAMs presenting tri(ehtyleneglycol) termianl groups were treated with matrix (2′,4′,6′-trihydroxyacetophenone , 5 μL, 5 mg/mL in anhydrous acetonitrile) dried, and inserted in MALDI-ToF MS to desorb the designated regions of SAMs. A 337 nm nitrogen laser was used as a desorption-ionization source, all desorption processes were carried out with 20 kV acceleration voltage using reflective mode in positive ion. The extraction delay time was 200 nsec. The patterned SAM substrates using MALDI-ToF MS were immediately rinsed with deionized water and ethanol, dried under a stream of nitrogen. The exposed gold surface by local desorption on the substrates was backfilled by immersing the substrates into 1 mM ethanolic solution of hexadecanethiol for 1 h. The substrates were rinsed with deionized water and ethanol and dried under a stream of nitrogen.

Droplet evaporation induced self-assembly of GNRs

GNRs with aspect ratio 2.1 was synthesized by seed growth method according to the procedure reported by Murphy and coworkers (Figure S1 in the Supporting Information).[30] A 10 μL of the colloidal suspension of GNRs was respectively applied on the substrates modified with various SAMs and evaporated at approximately 30% humidity and room temperature. After evaporation, the ordered assemblies of GNRs along the edges or whole area of droplets were observed on the substrates.

SERS experiments on ordered assemblies of GNRs

The ordered assemblies of GNRs formed on SAMs presenting different terminal groups were incubated in 1 mM ethanolic solution of 4-ATP for 12 h, washed with water and ethanol and dried under a stream of nitrogen. To estimate quantitative SERS enhancement, the ordered assemblies of GNRs were prepared on gold substrates (1 cm^2), briefly treated with piranha solution to remove organic layers on their surfaces and treated by 1 μL of 1 mM ethanolic solution of 4-ATP. The array of GNR ordered assemblies was fabricated by dropping GNR suspension on HDT functionalized surface with regular distance and treated with 1 μL of 0.1, 0.5 and 1.0 mM ethanolic solution of 4-ATP.

Characterization

UV-Vis-NIR spectrum of synthesized nanorod suspension was recorded by SPECTRA max Plus384 (Molecular Devices, U.S.A.). Contact angle measurements of water and GNR suspension were performed by Phoenix300 (S.E.O., Korea). The structures of GNR ordered assemblies were observed with a field emission SEM S-4800 (Hitachi, Japan) and BX51M optical microscope (Olympus Co., Japan). Two-photon luminescence was measured with a Zeiss LSM 510 NLO

integrated with Chameleon Ultra II (mode-locked Ti:Sapphire laser, pulse width < 140fs, wavelength = 800 nm) as a IR laser source. The laser was focused with a water-immersion objective (40 x, numerical aperture = 0.75). The laser power of 20.1 mW and band-pass filter (570 – 640 nm) were used for scanning. Raman characterization was carried out by LabRAM HR UV/vis/NIR (Horiba Jobin Yvon, France) using an 20 mW Ar ion CW laser (514.5 nm) as an excitation source focused through a BXFM confocal microscope equipped with an objective (50×, numerical aperture=0.50).

Results and discussion

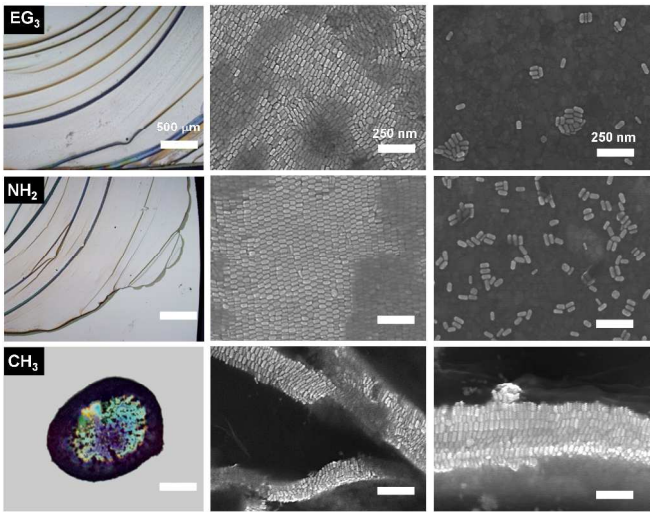

Fig. 1 Bright field image (first column), SEM images of ordered assembly structure at the edge (second column) and at the center (third column). The scale bars are 500 μm in bright field images and 250 nm in SEM images, respectively.

First, we prepared SAMs presenting various functional groups such as tri(ehtyleneglycol) (EG_3), primary amine (NH_2) and methyl (HDT, stands for hexadecane thiol) on gold coated substrates (for chemical structures of thiol derivatives, see Figure S2). The three different terminal groups were chosen to provide different surface environments (hydrophobic or hydrophilic) to control evaporation mode. We then applied 10 μL of colloidal GNRs (2.98 nM) on each SAM surface and evaporated the samples in ambient condition. Then, the assemblies of GNRs formed on the substrates were analyzed using a reflective optical microscope (OM) for low-magnification images, and a scanning electron microscope (SEM) for high-magnification images (Figure 1 and S3). The OM images showed multiple ring structures along the edge of the suspension droplets (created via the so-called "coffee ring" effect)[31] on EG_3 and NH_2 functionalized surfaces. Surprisingly, a large crystalline structure over 1.6 mm in diameter was formed on HDT functionalized surface instead of multiple ring structures. SEM images also showed similar results to OM characterization. The multiple narrow ring structures formed on EG_3 and NH_2 functionalized surfaces were composed with less-ordered GNRs than HDT functionalized surfaces. This result shows that ordered assembly on relatively hydrophilic surface only occurred at the droplet edges of colloidal GNRs by formation of multiple pinning points with successive slip-motions during constant area evaporation mode (Scheme 1c). Conversely, the large crystalline structure formed on highly hydrophobic HDT functionalized surface with highly ordered structure of GNRs (Figure 1). This interesting ordered assembly behaviour is attributed to droplet edge movement of colloidal GNRs during constant angle evaporation mode induced by the hydrophobic surface with 90° contact angle of colloidal droplet of GNRs. These results suggest that appropriate surface functionalization could result in a large scale ordered assembly of GNRs. As a demonstration of this concept, the evaporation induced assembly of GNRs was carried out on Si substrates that were functionalized with different moieties (Figure S4). We found that the assembly of GNRs could be mediated by surface engineering strategy on Si substrates in addition to gold coated substrates (Figure S5).

To quantitatively correlate the change of evaporation mode with substrate surface properties, contact angles of water and the colloidal suspension of GNRs, and the evaporation rate of them, were measured for each droplet on each substrate (Figure 2 and S6). These parameters closely related to the evaporation mode are important for successful large scale ordered assembly of GNRs since the formation of the liquid crystalline assembly is a function of rapid solvent evaporation and the resulting increased concentration of GNRs via convective flow at the edge of the droplet.[32,33] During constant area evaporation mode, GNRs in the droplet move toward droplet edge by convective flow to cause increased local concentration and form sequential pinned points with ordered structure by successive droplet slip-motion. Thus, formation of large crystalline structure is not possible. However, the ordered assembly process of GNRs during constant angle evaporation mode quite different from constant area evaporation mode because the droplet edge of colloidal GNRs keeps in fast moving toward inside of droplet with increased local concentration of GNRs throughout constant angle evaporation mode. Since this motion of the droplet edge is faster than the slip-motion of droplet edge during constant area evaporation mode, the diameter of suspension droplet on surface became smaller and smaller, before the concentration of GNRs reaches a critical point to form a pinning point, and thus a large crystalline structure was formed with well-ordered structure of GNRs.

Functional group	EG_3	HDT	NH_2
Contact angle of water	41	110	49
Contact angle of colloidal suspension of GNRs	34	90	36
Evaporation time (min)	42	52	45
Degree of order	Low	High	Medium

Fig. 2 The contact angles of water and nanorod suspension, evaporation time of nanorod suspension and degree of order in assembled structure of gold nanorods on SAMs presenting different functional groups.

We measured TPL of the assembled structures of GNRs. Previously, the TPL of GNRs with ordered structures was reported to be enhanced relatively to that with disordered structures.[13] We measured the TPL of assembled GNRs formed on EG_3, NH_2 and HDT functionalized surfaces which have different crystalline size in their ordered structures. The luminescence images and intensity profiles in Figure 3a show

that the intensity of TPL on SAMs presenting different terminal groups increased in order of EG_3 < NH_2 < HDT and the area emitting TPL is also quite large on HDT functionalized surface compared to the other surfaces due to the different size of their crystalline structures, which concurs with previous OM and SEM characterization results (Figure 3a). These results also demonstrate that a large scale ordered assembly of GNRs can be achieved by controlling substrate surface properties to pre-define evaporation mode of colloidal droplet of GNRs.

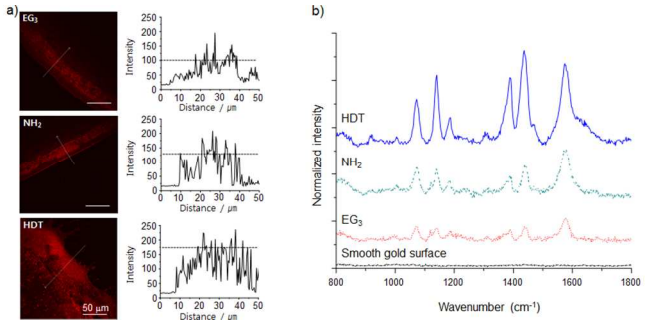

Fig. 3 Enhanced TPL images and intensity profiles of ordered assemblies of GNRs in their coffee ring regions formed at the edge of suspension droplets placed on various SAMs. b) Raman spectra of adsorbed 4-ATP on the smooth gold surface and ordered assemblies of GNRs formed on EG_3, NH_2, and HDT functionalized gold surfaces. The ordered assemblies were incubated in 1 mM ethanolic solution for 12 h. Spectral intensities of all spectra were normalized with Raman signal from smooth gold surface. The scale bars are 50 μm.

We carried out Raman analysis to investigate Raman signal enhancement of 4-aminothiophenol (4-ATP) on the ordered assemblies of GNRs formed on EG_3, NH_2 and HDT functionalized surfaces.[34] Prior to a SERS experiment, the ordered assemblies of GNRs were briefly treated by piranha solution to remove CTAB layer for homogenous adsorption of 4-ATP. Although this process resulted in the structural damage to the ordered assemblies of GNRs (Figure S7), it was required to acquire reliable and reproducible SERS spectra because the presence of organic layers on gold nanorods could interfere peaks of interest in SERS spectra (Figure S8).[35] The oxygen plasma or ozone treatments might be an alternative way to remove CTAB layer on GNRs without structural damage to maintain the number of nanogaps which might act as "hot spots" in their assembled structures for high SERS performance. The Raman spectra in Figure 3b showed negligible Raman signal on piranha treated smooth gold surface. On the other hand, the SERS peaks of 4-ATP at 1077, 1143, 1391, 1435 and 1577 cm^{-1} were observed on the ordered assemblies of GNRs. The different peak positions from that of bulk 4-ATP in Raman spectrum might be attributed to charge transfer phenomena (Figure S9).[36] Despite of structural damage of assembled GNRs, the ordered assembly structures still provide many "hot spots" in their structures. Therefore, the SERS signal intensities increased with the degree of order in assembled GNRs. It is well known that the multi-layered structure of GNRs shows significant Raman signal enhancement of benzene thiol derivatives adsorbed on their surfaces.[37] To quantitatively compare the SERS signal enhancement, the enhancement factor (EF) of 4-ATP on ordered assemblies of GNRs was estimated. The EF is generally defined as[38]

$$EF = I_{SERS}N_{bulk} / I_{Raman}N_{surface}$$

Where I_{SERS} and I_{Raman} are respectively the intensities of the peaks at 1577 cm^{-1} in SERS spectrum (Fig. 3b) and 1597 cm^{-1} normal Raman spectrum (Fig. S8), and N_{bulk} and $N_{surface}$ are respectively the number of 4-ATP molecules exposed to laser spot (1 μm in diameter) under SERS and normal Raman analysis condition (for detailed calculation, see Figure S10). Approximate EF values of 4-ATP on the ordered assemblies of GNRs formed on SAMs presenting EG_3, NH_2 and HDT were respectively determined as 1.1×10^3, 1.7×10^3 and 1.8×10^3 with 514 nm excitation source. These results well concur with TPL studies. The relatively low EF values could be attributed to the structural damages of GNRs in assembled structures induced by piranha treatment.

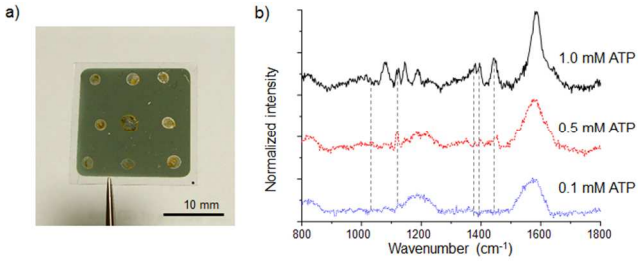

Fig. 4 a) Photograph of large crystalline structured gold nanorod array on HDT functionalized surface. b) The Raman spectra of different amounts of 4-ATP, 1.0, 0.5 and 0.1 nmol were obtained from the array of ordered assemblies of GNRs treated by spotting 1 μL of 1.0, 0.5 and 0.1 mM ethanolic solution of 4-ATP. The scale bar is 10 mm.

We next fabricated array of GNR assemblies on HDT functionalized surface. The constant contact angle evaporation mode on hydrophobic surface resulted in formation of large crystalline structure of GNRs in compact area by shrinkage of droplet on surface. Therefore, array of large crystalline structure of GNRs was successfully fabricated on a HDT functionalized surface (Figure 4a). The each spot of array was treated by 1.0, 0.5 and 0.1 nmol of 4-ATP in ethanol and allowed to be dried under ambient condition. The Raman signal intensities obtained on those spots of ordered GNR assemblies was dependent on the concentration of 4-ATP solutions. The trace amount of 4-ATP, approximately 0.5 nmol, was detected on the ordered assembly of GNRs due to the strong enhancement of Raman signal (Figure 4b). This array of ordered GNR assemblies could be a novel platform for fabrication of SERS based biochips and sensors.

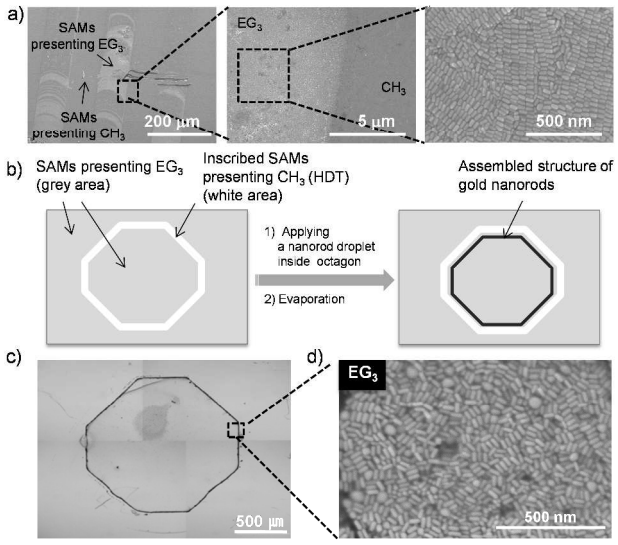

Fig. 5 a) SEM images of patterned assembly of gold nanorods fabricated by solvent-evaporation on stripe-patterned SAMs presenting HDT and EG_3 groups. b) Strategy to inscribe methyl terminal groups at designated region among SAMs presenting EG_3 terminal groups for confined evaporation of a colloidal droplet of GNRs inside octagon. c) Bright field (first column) and (d) SEM images of octagon patterned assemblies of GNRs fabricated by droplet evaporation on pre-patterned SAMs presenting methyl terminal groups among EG_3 terminal groups.

We next carried out droplet evaporation induced self-assembly of GNRs on a substrate patterned with alternating stripes of hydrophobic and hydrophilic regions. The SAMs presenting EG_3 were chosen as hydrophilic modifiers since EG_3 terminal group exhibited significantly different evaporation mode compared to SAMs presenting HDT terminal groups. Line patterns were first fabricated on gold-coated substrates by microcontact printing of HDT and followed back-filling of alkanethiols presenting EG_3 terminal group.[39] Water droplets, when placed on microscale line patterns with alternating hydrophilic and hydrophobic regions, create a contorted wetting line.[40] During the evaporation process, the colloidal droplet of GNRs that had been placed on the patterned surface exhibited a wetting line on EG_3-back-filled regions. Therefore, ordered assemblies of GNRs were only formed on EG_3-patterned regions along the movement of droplet edge of colloidal GNRs (Figure 5a).

Then, we carried out droplet evaporation induced self-assembly of GNRs along pre-designated shape fabricated by utilizing mass spectrometry-assisted lithography (MASSAL) on a substrate.[41] We first prepared SAMs presenting EG_3 terminal groups on a gold coated substrate. The patterning process started with selectively removing SAMs presenting EG_3 terminal groups along an octagonal shape on the gold coated substrate by local laser irradiation with a laser equipped with MALDI-ToF MS. The substrate was then backfilled with HDT. This process yielded a hydrophobic octagonal line inscribed on hydrophilic SAMs presenting EG_3 terminal groups (Figure 5b). Therefore, a droplet of colloidal GNRs applied inside the octagon pattern would be restricted in shape and size by the physical constraints of the HDT octagonal line (Figure 5c). Evaporation of the droplet then results in the deposition of ordered assemblies of GNRs along the HDT octagon line (Figure 5d).

Conclusions

A new strategy to fabricate large scale and pre-designed ordered assembly of GNRs was developed as a SERS platform. This work is based on substrate surface modification as a means to modulate surface properties that influence droplet evaporation mode. Both the large scale ordered assembly of GNRs and its array formation were achieved by simply changing the functionality of the substrate surface. The present study is the first example of a systematic investigation showing the effect of substrate surface properties on ordered assemblies of GNRs. Furthermore, these surface properties were tailored to fabricate the assemblies in an array format for SERS. This new strategy can be further implemented in the construction of well-ordered structures and for fabricating various patterns containing the characteristic collective physical properties of other nanomaterials. In a parallel series of experiments, the applicability of the present nanostructure patterning strategy is being examined for the fabrication of surface plasmon-based sensors and functional biochips.

Acknowledgements

This work was supported by the Basic Science Research Program (2011-0017356) through the National Research Foundation of Korea (NRF) and by the Research Center Program (EM1402) of Institute for Basic Science (IBS) funded by the Korean government.

Notes and references

[a] Center for RNA Research, Institute for Basic Science, Department of Chemistry, Seoul National University, Seoul, 151-747, Republic of Korea
E-mail: dalheemin@snu.ac.kr.

† Electronic Supplementary Information (ESI) available: The detailed experimental procedure and additional data. See DOI: 10.1039/b000000x/

1 X. Hu, W. Cheng, T. Wang, Y. Wang, E. Wang, S. Dong, *J. Phys. Chem. B* 2005, **109**, 19385.
2 A. V. Kabashin, P. Evans, S. Pastkovsky, W. Hendren, G. A. Wurtz, R. Atkinson, R. Pollard, V. A. Podolskiy, A. V. Zayats, *Nat. Mater.* 2009, **8**, 867.
3 P. Reineck, G. P. Lee, D. Brick, M. Karg, P. Mulvaney, U. Bach, *Adv. Mater.* 2012, **24**, 4750.
4 L. Y. Pan, Y. L. Zhang, H. Y. Wang, H. Liu, J. S. Luo, H. Xia, L. Zhao, Q. D. Chen, S. P. Xu, B. R. Gao, L. M. Fu, H. B. Sun, *Nanoscale* 2011, **3**, 2882.
5 N. N. Khanh, K. B.Yoon, *J. Am. Chem. Soc.* 2009, **131**, 14228.
6 J. Zhou, B. Duan, Z. Fang, J. Song, C. Wang, P. B. Messersmith, H. Duan, *Adv. Mater.* 2014, 26, 701.
7 J. Bahadur, D. Sen, S. Mazumder, B. Paul, H. Bhatt, S. G.Singh, *Langmuir* 2012, **28**, 1914.
8 H. P. Zhou, C. Zhang, C. H. Yan, *Langmuir* 2009, **25**, 12914.
9 P. K. Jain, S. Eustis, M. A. El-Sayed, *J. Phys. Chem. B* 2006, **110**, 1824.

10 G. A. Wurtz, P. R. Evans, W. Hendren, R. Atkinson, W. Dickson, R. J. Pollard, A. V. Zayats, W. Harrison, C. Bower, *Nano Lett*. 2007, **7**, 1297.
11 A. M. Funston, C. Novo, T. J. Davis, P. Mulvaney, *Nano Lett*. 2009, **9**, 1651.
12 B. Peng, G. Li, D. Li, S. Dodson, Q. Zhang, J. Zhang, Y. H. Lee, H. V. Demir, X. Y. Ling, Q. Xiong, *ACS Nano* 2013, **7**, 5993.
13 T. Ming, X. Kou, H. Chen, T. Wang, H. L. Tam, K. W. Cheah, J. Y. Chen, J. Wang, *Angew. Chem. Int. Ed.* 2008, **47**, 9685.
14 C. J. Orendorff, P. L. Hankins, C. J. Murphy, *Langmuir* 2005, **21**, 2022.
15 Z. Sun, W. Ni, Z. Yang, X. Kou, L. Li, J. Wang, *Small* 2008, **4**, 1287.
16 T. S. Sreeprasad, A. K. Samal, T. Pradeep, *Langmuir* 2008, **24**, 4589.
17 Y. Xie, S. Guo, C. Guo, M. He, D. Chen, Y. Ji, Z. Chen, X. Wu, Q. Liu, S. Xie, *Langmuir* 2013, **29**, 6232.
18 A. Gole, C. J. Murphy, *Langmuir* 2005, **21**, 10756.
19 Z. Nie, D. Fava, E. Kumacheva, S. Zou, G. C. Walker, M. Rubinstein, *Nat. Mater*. 2007, **6**, 609.
21 K. Mitamura, T. Imae, N. Saito, O. Takai, *J. Phys. Chem. B* 2007, **111**, 8891.
22 Z. Nie, D. Fava, M. Rubinstein, E. Kumacheva, *J. Am. Chem. Soc*. 2008, **130**, 3683.
23 J. Xiao, Z. Li, X. Ye, Y. Ma, L. Qi, *Nanoscale* 2014, **6**, 996.
24 A. Ulman, *Chem. Rev.* 1996, **96**, 1533.
25 A.K. Cheng, D. M. Soolaman, H. Z. Yu, *J. Phys. Chem. B* 2006, *110*, 11267.
26 A. K. Cheng, D. M. Soolaman, H. Z. Yu, *J. Phys. Chem. B* 2007, **111**, 7561.
27 K. S. Birdi, D. T. Vu, *J. Adhesion Sci. Technol.* 1993, **7**, 485.
28 H. Z. Yu, D. M. Soolaman, A. W. Rowe, J. T. Banks, *Chemphyschem* 2004, **5**, 1035.
29 C. Pale-Grosdemange, E. S. Simon, K. L. Prime, and G. M. Whitesides, *J. Am. Chem. Soc.* 1991, **113**, 12.
30 T. K. Sau, C. J. Murphy, *Langmuir* 2004, **20**, 6414.
31 R. D. Deegan, O. Bakajin, T. F. Dupont, G. Huber, S. R. Nagel, T. A. Witten, *Nature* 1997, **389**, 827.
32 A. P. Sommer, N. Rozlosnik, *Cryst. Growth Des*. 2005, **5**, 551.
33 J. Lim, W. Lee, D. Kwak, K. Cho, *Langmuir* 2009, **25**, 5404.
34 The detailed peak assignment has been reported elsewhere and will not be described here because this experiment is focused on Raman signal enhancement. For detailed information, see Y. M. Lee, K. K, K. S. Shin, *J. Phys. Chem. C* 2008, **112**, 10715.
35 S. Yun, Y. K. Park, S. K. Kim, S. Park, *Anal. Chem.* 2007, **79**, 8584.
36 M. Osawa, N. Matsuda, K. Yoshii, I. Uchida, *J. Phys. Chem.* 1994, **98**, 12702.
37 S. Lee, L. J. Anderson, C. M. Payne, J. H. Hafner, *Langmuir* 2011, **27**, 14748.
38 Y. –K. Kim, D. –H. Min, *RSC adv*. 2014, **4**, 6950.
39 M. Mrksich, G. M. Whitesides, *Annu. Rev. Biophys. Biomol. Struct.* 1996, **25**, 55.
40 J. Drelich, J. L. Wilbur, J. D. Miller, G. M. Whitesides, *Langmuir* 1996, **12**, 1913.
41 Y. –K. Kim, S. –R. Ryoo, S. –J. Kwack, D. –H. Min, *Angew. Chem. Int. Ed.* 2009, **48**, 3507.

